Limits of stability of the liquid phase in a lattice model with water-like properties

Srikanth Sastry
Center for Polymer Studies and Department of Physics, Boston University, Boston, Massachusetts 02215

Francesco Sciortino
Center for Polymer Studies and Department of Physics, Boston University, Boston, Massachusetts 02215 and CRS4, Centro di Ricerca, Sviluppo e Studi Superiori in Sardegna, P. O. Box 488, 09100 Cagliari, Italy

H. Eugene Stanley
Center for Polymer Studies and Department of Physics, Boston University, Boston, Massachusetts 02215

(Received 30 October 1992; accepted 1 March 1993)

Explicit study of the hydrogen bond network in water offers a *microscopic* approach to understanding the anomalous properties of water, while an alternate, *thermodynamic* approach is offered by the reentrant limit of stability (spinodal) conjecture. To relate the two approaches, we develop a lattice model based on microscopic considerations. We show that the model displays anomalous thermodynamic behavior that is in qualitative agreement with the behavior of water. We study the model in the mean field approximation and by numerical simulations. We explicitly demonstrate the interrelation between density maxima and the reentrance of the spinodal: both originate from the contribution of orientational degrees of freedom to the thermodynamics of the system. The metastable liquid state is bounded by a spinodal at positive pressures as well as negative pressures, where the positive pressure spinodal is the limit of stability with respect to the solid state. The liquid–gas and liquid–solid spinodals form a continuous locus, but the "critical" properties of these two spinodals are quite different. While the response functions (specific heat, compressibility) diverge at liquid–gas spinodal, at the liquid–solid spinodal they do not—even though the response functions tend to higher values in the same fashion as occurs near the liquid–gas spinodal.

I. INTRODUCTION

Water, in the liquid phase, exhibits well-known anomalous behavior for a wide range of temperatures and pressures close to the coexistence line with the solid phase, such as the density maximum at 4 °C at atmospheric pressure, the isothermal compressibility minimum at 46 °C, and the rise upon cooling of the constant pressure specific heat. This anomalous behavior extends into the metastable region of the liquid and has been particularly well studied in the supercooled state, where these anomalies grow stronger.[1] Experimental studies are, however, limited in the metastable region by homogeneous nucleation (whereby the stable phase of the system grows spontaneously) and by the challenge of attaining large negative pressures.[2]

From a microscopic point of view, theoretical and experimental studies have established that the anomalous properties of water are related to the hydrogen bond network. Hence, microscopic approaches to explaining anomalies in water focus on the properties of this hydrogen bond network. An attempt to view the problem from a different perspective was initiated by Speedy and Angell,[3] who observed that at atmospheric pressure, various thermodynamic quantities appear to diverge at a single temperature T_s below the homogeneous nucleation temperature T_N. They proposed that T_s corresponds to the absolute limit of stability (the spinodal) for the liquid and, further, that the locus of limits of stability for the liquid forms a continuous curve. Speedy[4] showed that from the assumed shape of the limit of stability line, the thermodynamic anomalies of water—including the existence of a density maximum—could be deduced. The spinodal line estimated by Speedy turns around at a temperature of 35 °C and a pressure of −210 MPa, upon intersecting the line of density maxima, and reaches positive pressures at −45 °C. Speedy's *thermodynamic* analysis has been generalized by Debenedetti *et al.*,[5] who derive relations for any liquid between density anomalies and spinodal behavior from requirements of thermodynamic consistency.

However, in spite of much work on the issue,[4–6] the stability limit conjecture of Speedy and Angell remains unsettled. In particular, the conjecture has not been addressed by studies of the microscopic behavior of water. In order to understand the relationship between the microscopic causes of anomalies and the behavior of the limits of stability, we introduce a lattice-gas model based on the microscopic properties of water. Various lattice models have been studied previously,[7,8] but generally,[9] insufficient attention has been paid to the study of the metastable behavior, which is the focus of this paper. We obtain thermodynamic behavior that is in qualitative agreement with the behavior of water. We explicitly demonstrate the relationship between anomalous density behavior and the behavior of the limits of stability, both being obtained from a common microscopic mechanism. We show that at low

 0021-9606/93/129863-10$06.00

temperatures the liquid–gas spinodal merges with and gives way to the liquid–solid spinodal line, which becomes the physically relevant limit of stability. Thus, the reentrance of the spinodal does not imply that the liquid becomes unstable at low temperatures to gas-like fluctuations. The low-temperature fluctuations are the same that prompt the formation of the open ice structure.

II. MOTIVATION FOR THE MODEL

From the interpretation of experimental data,[10] as well as from detailed microscopic results provided by computer simulations,[11–14] liquid water is viewed as an imperfect network of hydrogen bonds: regions with strong linear hydrogen bonds intercalate with regions of distorted hydrogen bonds. While the low energy regions are characterized by tetrahedral coordination and a local density comparable with that of ice, the weakly bonded regions are characterized by a higher local density and by higher molecular mobility. In typical configurations the molecules in high density regions have more than four neighbors in their first coordination shell, and significantly larger orientational entropy compared to molecules in the low density region.[14] Thus, the gain in orientational entropy serves to stabilize the higher density (and higher energy) configurations with respect to energetically more favorable low density structures. A reflection of this mechanism is the persistence of the liquid state, even at temperatures at which the hydrogen bond energy is considerably larger than the thermal energy.

The above description of the liquid phase suggests that the transition from the solid to the liquid phase is driven by the *rotational entropy* gain associated with configurations of higher local density. Conversely, if we start at high temperatures where water behaves normally, similar considerations can explain the onset of anomalous behavior as the temperature is lowered; indeed, orientational entropy considerations are implicit in earlier work which describe water anomalies in terms of an increase in the concentration of four-bonded molecules,[15] unstrained polyhedral species[16] or pentagonal ring structures[17]—all of which locally reduce the entropy and also the density. The formation of these specific structures as the temperature is reduced can be interpreted as the weakening of the entropic advantage of higher density states.

Thus, the inclusion of the entropic contribution associated with high density configurations is important for describing the behavior of water. Our purpose here is to develop a simple lattice-gas model incorporating these considerations.

III. THE MODEL

The basic features we want the model to incorporate are the following.

(1) The low temperature state (ground state) of the system should have an open, low density structure like that of ice.

(2) Linear hydrogen bonds can form between two molecules only when (a) the local configuration is open and (b) the participating molecules are properly oriented.

(3) Increased local density with respect to the open structure must result in an increase in the (a) local energy and (b) the local entropy. The normal lowering of energy on increasing the number of neighbors is reversed in water due to the distortion of hydrogen bonds.

We describe the Hamiltonian constructed from these considerations in two steps. Also, for simplicity, we describe the model for a two-dimensional square lattice. The corresponding three-dimensional lattice will be described at the end of this section.

In the first step, we define a Hamiltonian that has, as its ground state, a low density configuration, with an open structure. We define an occupancy variable n_i ($n_i = 0$ or 1) for each lattice site i. If $n_i = 1$, lattice site i is said to be occupied by a molecule. If $n_i = 0$, lattice site i is empty.

In order to define the open structure, we partition the lattice into two interpenetrating sublattices, A and B, as shown in Fig. 1(a). In the ground state configuration, one sublattice is completely occupied and the other is empty. The Hamiltonian $\mathscr{H}_1$ that describes such a ground state favors the occupation of adjacent sites on the same sublattice (AA or BB pairs) and disfavors the occupation of adjacent sites on different sublattices (AB pairs). Thus we define

$$\mathscr{H}_1 \equiv -2\epsilon \sum_i \left(\sum_k^{(AA)} n_i n_k + \sum_j^{(AB)} n_i n_j \right) - 2J \sum_i \sum_j^{(AB)} n_i (1-n_j). \tag{1}$$

Here $\Sigma_i \equiv \Sigma_{i=1}^N$ denotes the sum over *all* sites in the lattice, $\Sigma_k^{(AA)}$ is the sum over the z neighbors of site i on the same sublattice, and $\Sigma_j^{(AB)}$ is the sum over the z neighbors of site i on the other sublattice (if i is on sublattice A, j is on sublattice B and vice versa).[18]

The first term in (1) describes normal liquid behavior, where the energy is proportional to the number of interactions. The second term describes the *extra* energy (if $J > \epsilon$) gained by the formation of a linear hydrogen bond in the open structure, where sites on only one of the sublattices are occupied.[19] Thus, in the ground state, each occupied site has z interactions with occupied sites and contributes an interaction energy of $-2z(J+\epsilon)$. If we associate with each pair of occupied sites a "hydrogen bond," then the energy of a single hydrogen bond is $-4(J+\epsilon)$.

The Hamiltonian (1) satisfies all the conditions stated above, except 2(b) and 3(b), both of which refer to the orientational state of molecules. Since the model Hamiltonian $\mathscr{H}_1$ so far contains no orientational degrees of freedom, (i) the hydrogen bond is not yet defined subject to any condition on the orientational state, and (ii) when the local density increases by the occupation of an AB neigh-

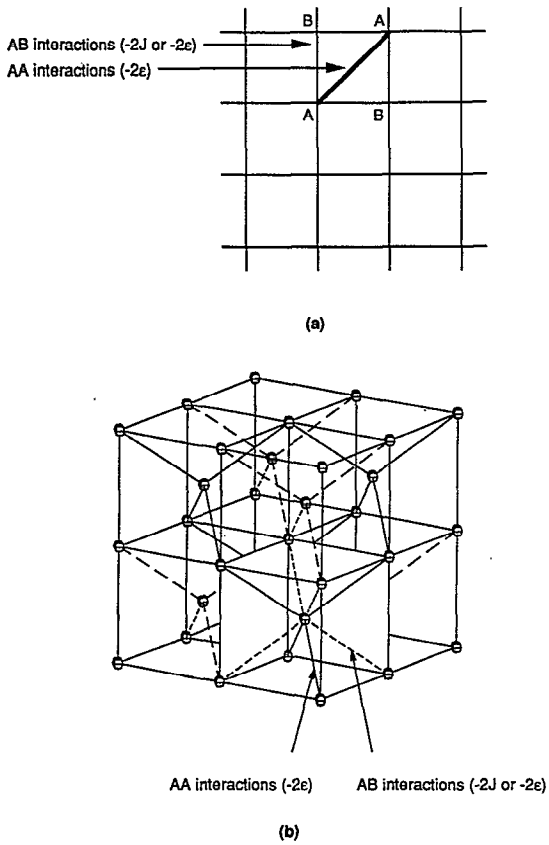

FIG. 1. The division of the lattice into sublattices (A, B) and interactions of sites of the same sublattice (AA interactions) and different sublattices (AB interactions) are shown (a) for the two-dimensional square lattice, and (b) for the three-dimensional bcc lattice. The A sites are connected by solid diagonal lines to form one of the diamond sublattices. The B sites are connected by long dashed diagonal lines to form the other sublattice. Note that sites at the center of two adjacent cubes belong to different diamond sublattices. The short dashes in the lower right cube indicate AB interactions and should not be confused with the lines representing the division into sublattices. The AA interaction strength is always -2ϵ while the AB interaction strength is -2ϵ or $-2J$ depending on the orientational state of the molecule.

bor, there is no increase in entropy. Therefore we extend $\mathscr{H}_1$ to incorporate such orientational degrees of freedom.

First, we must describe the orientational state of a molecule. We follow the spirit of Ref. 24 and associate with each *occupied* site i an additional (Potts) variable, σ_i, which can take values between 1 and q ($\sigma_i = 1,2,\ldots,q$). We distinguish "bonding" from "nonbonding" orientations by associating a subset of possible values of σ_i with orientations in which hydrogen bonding can take place. It is sufficient to choose this subset to be one specific value of σ_i, namely $\sigma_i = 1$, since what is significant is the ratio of degeneracies of bonding and nonbonding orientations.

To include this orientational information, the extra energy corresponding to the second term in (1) is present if and only if the occupied site i is in the properly oriented state, $\sigma_i = 1$. To achieve this, we *multiply* the second term in (1) by $\delta_{\sigma_i 1}$, which is zero when $\sigma_i \neq 1$. With this modification, (1) becomes

TABLE I. (a) Possible AA pair configurations and their interaction energies. (b) Possible AB pair configurations and their interaction energies.

n_i	n_j	Energy
1	0	0
0	1	0
0	0	0
1	1	-2ϵ

n_i	σ_i	n_j	Energy
1	$\neq 1$	0	0
0		0	0
0		1	0
1	Any	1	-2ϵ
1	1	0	$-2J$

$$\mathscr{H}_2 = -2\epsilon \sum_i \left(\sum_k^{(AA)} n_i n_k + \sum_j^{(AB)} n_i n_j \right) - 2J \sum_i \sum_j^{(AB)} n_i (1-n_j) \delta_{\sigma_i 1}. \tag{2}$$

The interaction energies for all the AA and AB pair configurations with the relevant orientational information are summarized in Table I. Two noteworthy features are (i) the orientational state affects the interaction energy only of an AB pair of occupied and empty sites; (ii) since in such an AB pair configuration only one site is occupied, $\mathscr{H}_2$ does not contain any interaction term between the variables σ_i. The inclusion of orientational degrees of freedom in this manner is sufficient to give rise to a difference between the orientational entropies of "hydrogen bond" interactions and other interactions.[20]

We illustrate the behavior of the system defined by the Hamiltonian (2) by inspecting the ground state of the system and some excitations above this ground state. In the ground state, only one of the sublattices (say A) is occupied, and each occupied site i is in the orientational state $\sigma_i = 1$. This configuration is shown in Fig. 2(a). The energy per occupied site is $-2z(J+\epsilon)$ with $z=4$.

As illustrations of the behavior of the system, we consider excitations arising from changing the state of the system at one site, which can be of three types: (i) removing a molecule; (ii) adding a molecule; and (iii) changing the orientational state of a molecule. In all the three examples, the energy of the system increases. In case (i), the increase in energy is $2z(J+\epsilon)$ [Fig. 2(b)]. In case (ii), the energy increases by $2z(J-\epsilon)$, since the AB interaction energy changes from J to ϵ [Fig. 2(c)]. Also, in case (ii), the entropy increases by $k_B \log(q)$, since the added molecule can be in any of the q orientational states.[21] For case (iii), when the orientational state of a molecule changes, the increase in energy is $2zJ$ and the increase in entropy is $k_B \log(q-1)$ [Fig. 2(d)].[22]

The partition function written for $\mathscr{H}_2$ can, in the first approximation, be reduced to an effective lattice-gas partition function by performing an approximate sum over the orientational degrees of freedom.[23] In the resulting effective Hamiltonian, the AB interaction strength $J_1^{\text{eff}}(T)$ is

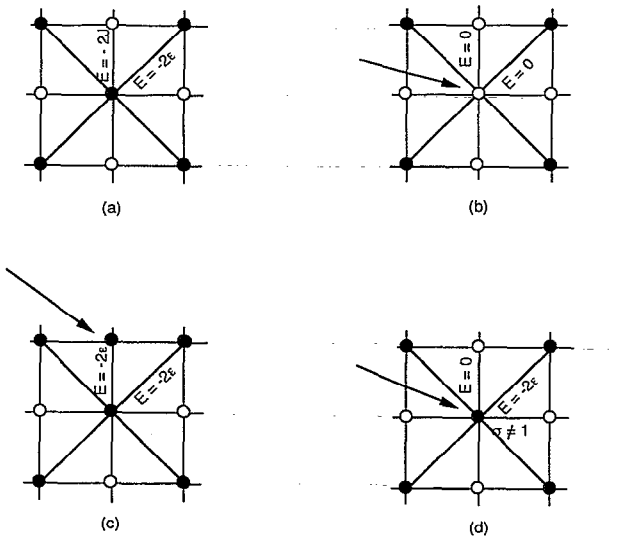

FIG. 2. The ground state configuration and three types of excitations that can occur over the ground state configuration. Only those diagonal bonds connecting to the central site are shown. The energies of interaction are indicated for an AB and an AA interaction between the central site and a neighboring site. (a) *The ground state.* Only one sublattice is occupied (filled circles) and all molecules are properly oriented for hydrogen bond formation ($\sigma_i = 1$). (b) *Removing a molecule.* The site where the molecule is removed is indicated by an arrow. The energy change is equal to the energy per site in the ground state, $2z(J+\epsilon)$. (c) *Adding a molecule.* The energy increase results from the change in interaction with surrounding neighbors from $-2J$ to -2ϵ [cf. with (a)]. The entropy increase is $\log q$. (d) *Changing the orientational state of a molecule* ($\sigma_i \neq 1$). The interaction energy with neighboring sites changes from $-2J$ to zero. The entropy increase is $\log(q-1)$.

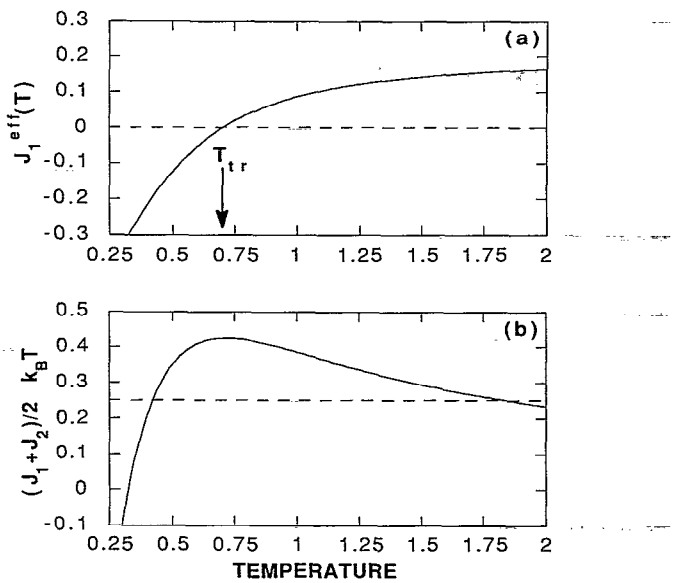

FIG. 3. (a) The effective AB interaction strength $J_1^{\text{eff}}(T)$ as a function of temperature (solid line). The dashed line corresponds to the value zero. The sign of the interaction changes at the temperature where the two lines cross. The temperature and the effective interaction are expressed in units of J. (b) $(J_1 + J_2)/2k_BT$ as a function of temperature (solid line). Also shown is the value of $1/z$ (dashed line). The two points of intersection correspond to critical points for liquid–gas coexistence.

temperature-dependent, since it contains information about behavior resulting from the orientational degrees of freedom. This effective Hamiltonian is given by

$$\mathcal{H}_3 = -2J_1^{\text{eff}}(T)\sum_i \sum_j^{(AB)} n_i n_j - 2\epsilon \sum_i \sum_k^{(AA)} n_i n_k - [z\delta J(T) + k_B T \log q]\sum_i n_i. \tag{3}$$

Here,

$$J_1^{\text{eff}}(T) \equiv \epsilon - \frac{\delta J(T)}{2} \tag{4}$$

is the effective AB interaction strength, while

$$\delta J(T) \equiv T \log\left[1 + \frac{1}{q}(e^{2J/k_BT} - 1)\right] \tag{5}$$

results from the approximate sum over variables σ_i in the last term of (2).

The temperature dependence of the coupling J_1^{eff} is shown in Fig. 3(a) for $J=1$, $\epsilon=0.3$ and $q=12$. These values will be used henceforth. At high temperatures, where the entropic effects dominate, the effective interaction approaches $\epsilon - J/q$ since the orientational degeneracy for this interaction is high. As the temperature decreases, the effective coupling moves away from this value, eventually crossing over to the opposite sign and approaching $\epsilon - J$ as T approaches zero. We denote the temperature where the effective coupling is zero by T_{tr}.

Although here we carry out calculations within the framework of a lattice model, the notion of a temperature-dependent interaction does not depend upon a lattice model. That is, without reference to a lattice, we can understand how a temperature-dependent interaction arises by noting that in a system where directional interactions are present, at high T the entropically favorable weak interactions are dominant in determining the effective interactions, while as T is lowered, the energetically favorable directional interactions become dominant. Thus, as T is varied, there is an effective change in the interaction.

Before concluding this section, we define the model in three dimensions. We consider a bcc lattice [Fig. 1(b)], which can be subdivided into two diamond lattices A and B by assigning to the two sublattices alternating sites on each of the interpenetrating cubic lattices. Thus, any given site is surrounded by eight sites (at the vertices of the surrounding cube), four of which belong to one sublattice and four to the other. We define nonzero interactions between each site and the sites on the surrounding cube. We define as before the interactions between sites belonging to the same sublattice (AA interactions) and between sites belonging to different sublattices (AB interactions). The model defined by these interactions exhibits the same phase behavior as the two-dimensional model above, and has a ground state with one of the diamond sublattices occupied and the other vacant.

IV. MEAN FIELD APPROXIMATION

In this section, we study the effective Hamiltonian $\mathscr{H}_3$ in the mean field approximation. The grand canonical partition function for the Hamiltonian (3) is

$$\Xi \equiv \exp\left(\frac{-\Omega}{k_B T}\right) \equiv \exp\left(\frac{PV}{k_B T}\right) = \sum_n \exp\left(\frac{-\mathscr{H}_3 + \mu N_o}{k_B T}\right). \quad (6)$$

Here $\Sigma_n \equiv \Sigma^1_{n_1=0} \cdots \Sigma^1_{n_N=0}$ is over all configurations of the occupancy variables n_i, N_o is the number of occupied sites in a given configuration, μ is the chemical potential, Ω the grand potential, and the volume V (on the left-hand side) given by the number of sites in the lattice. Making the standard mean field approximation for the grand potential, we write

$$\Omega = -PV = V\left[-zJ_1 n_A n_B - \left(\frac{zJ_2}{2}\right)(n_A^2 + n_B^2) - \left(\frac{\mu'}{2}\right)(n_A + n_B)\right] - T(S_A + S_B), \quad (7)$$

where n_A, n_B are the A and B sublattice densities and $\mu' = \mu + z\delta J + k_B T \log(q)$. The interaction strengths J_1 and J_2 are given by $J_1 \equiv 2\epsilon - \delta J$ and $J_2 = 2\epsilon$. S_A, the configurational entropy for molecules on sublattice A, is

$$S_A = -k_B(V/2)\,[n_A \log(n_A) + (1-n_A)\log(1-n_A)]. \quad (8)$$

The configurational entropy S_B for sublattice B is given by a similar expression.

In the mean field approximation, the stable solution is given by the values of n_A and n_B such that Ω is a minimum. For $T > T_{tr}$, both J_1 and J_2 are greater than zero. Thus, to find the stable solution, we can look for the minimum Ω in the (n_A, n_B) plane along the line defined by $n_A = n_B = n$, where n is the density. For $T < T_{tr}$ the search for the stability of the mean field solution must be performed in the entire plane, as described below.

For $T > T_{tr}$, the grand potential becomes

$$\Omega = V\{-z(J_1+J_2)n^2 - \mu' n + k_B T[n \log(n) + (1-n)\log(1-n)]\}. \quad (9)$$

The solution for the density n is given by the condition

$$\frac{1}{V}\frac{\partial \Omega}{\partial n} = 0 = -2z(J_1+J_2)n - \mu' + k_B T \log\left[\frac{n}{1-n}\right]. \quad (10)$$

Equation (10) is the familiar Bragg–Williams solution for the lattice gas, except that now the interaction strength is T dependent. The equation of state is the implicit equation

$$P_{eq} = -z(J_1+J_2)n_{eq}^2 - k_B T \log(1-n_{eq}), \quad (11)$$

where P_{eq} is the equilibrium pressure and n_{eq} is the equilibrium density.

To locate the critical point(s), we solve simultaneously

$$\left(\frac{\partial P}{\partial n}\right)_{T=T_c} = 0, \quad (12a)$$

$$\left(\frac{\partial^2 P}{\partial n^2}\right)_{T=T_c} = 0, \quad (12b)$$

with P given by (11). Equations (12) state that the P–V isotherm for $T = T_c$ is characterized by a horizontal tangent and an inflection point when $P = P_c$ and $n = n_c$. The solution of Eqs. (12) gives

$$k_B T_c = z(J_1+J_2)/2, \quad n_c = 1/2. \quad (13)$$

Thus, n has solutions other than $n = 1/2$ (the disordered solution above the critical point) if $z(J_1 + J_2)/2k_B T > 1$ or, equivalently, if $(J_1 + J_2)/2k_B T > 1/z$.

The temperature at which $(J_1 + J_2)/2k_B T = 1/z$ defines the critical point(s) for the liquid–gas transition, below which phase separation occurs. Figure 3(b) shows $(J_1 + J_2)/2k_B T$ plotted against temperature, as well as the quantity $1/z$. Notice that $(J_1 + J_2)/2k_B T$ cuts $1/z$ at two values, implying that the liquid–gas phase separation region is bounded by two critical points, an upper and a lower one.[24] The density of the liquid phase is 1/2 at both critical points, implying that the density must pass through a maximum between the two critical points. The model displays a density maximum which is closely connected to the existence of two critical points. Interestingly, both the critical points appear at positive pressure, given by $P_c = k_B T_c[\log(2) - 0.5]$. Note also that the lower critical point is below T_{tr}, since $k_B T_{tr} = 0.703$ for the choice of parameters mentioned above. As we shall see, the ordering behavior of the system changes below T_{tr}, and hence, the lower critical point is not in the stable region.

To calculate the equilibrium liquid–gas line we use the equal-area construction, while we use the equation of state (11) together with Eq. (12a) to calculate the spinodal line for the liquid–gas transition. For lower temperatures, the stability of solutions for which n_A is different from n_B must be investigated to define the correct coexistence lines. Similarly, the limit of stability calculated from Eq. (12a) could be pre-empted by instabilities in a direction perpendicular to the $n_A = n_B$ line, as discussed further in the following section.

At T_{tr}, the first neighbor coupling J_1 changes sign, so below T_{tr} we have *repulsive AB* and *attractive AA* interactions. In the Ising model mapping of the lattice gas, these interactions define a metamagnet.[25] Metamagnets have an ordered antiferromagnetic (AF) state below the Néel temperature. Antiferromagnetic order in the metamagnet corresponds to the low-density open structure in the lattice-gas system defined here. We shall refer to this low density ordered phase as the solid phase or ice.[26] To discuss the solid phase as well as the liquid and gas phases, we need to consider Eq. (7), the grand potential expressed in terms of the sublattice densities. The equilibrium solution for the solid phase is then obtained by solving simultaneously extremum conditions [like (10)] with respect to the two sublattice densities.

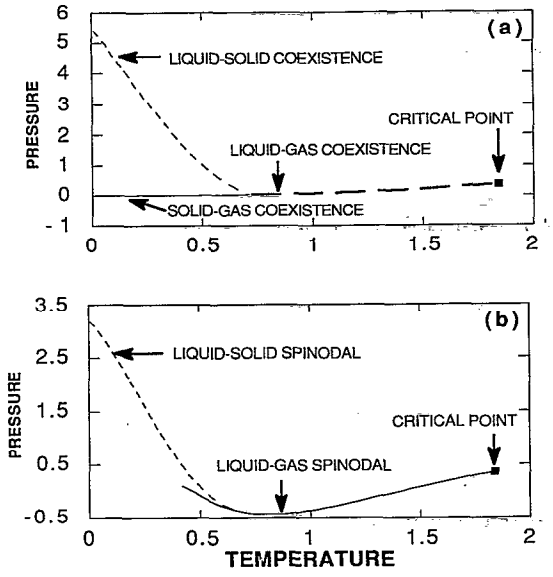

FIG. 4. (a) The phase diagram of the model. The coexistence lines between solid, liquid and gas phases are shown. The critical point for the liquid–gas transition is also shown. The pressure is expressed in arbitrary units. (b) The spinodals bounding the liquid phase. Note that the two lines meet smoothly at the triple point temperature.

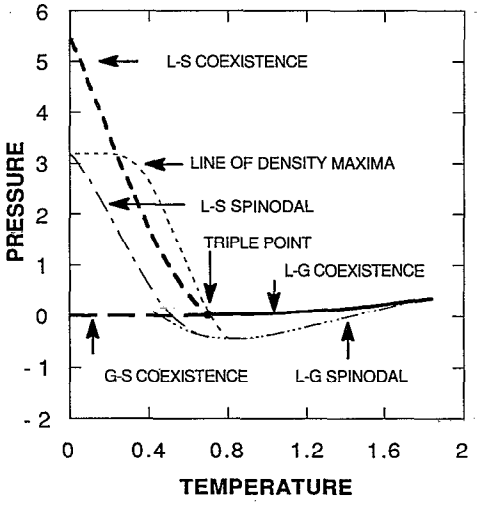

FIG. 5. Coexistence lines, spinodal boundaries of the liquid and the line of density maxima in the liquid phase. Note that the line of density maxima meets the liquid–gas spinodal at the point of reentrance, and meets the liquid–solid spinodal at zero temperature.

The equilibrium phase boundaries between the solid and the liquid/gas phases are found by comparing the grand potential for the respective solutions, the phase boundary being given by the condition that the grand potential Ω for the two phases be the same.

We then have three coexistence lines, one between the upper critical point for the liquid–gas transition and T_{tr}, and two coexistence lines between solid and liquid or gas phases, respectively. These three coexistence lines meet at T_{tr}. Since at T_{tr} we have three-phase coexistence, we identify (T_{tr},P_{tr}) as the triple point. Figure 4(a) shows the coexistence lines in the P–T plane. Note that the liquid–solid coexistence line has the negative slope expected for water at lower pressure values.[27]

V. LIMITS OF STABILITY AND THE LINE OF DENSITY MAXIMA

The limits of stability of the liquid phase can be obtained by locating the values of temperature and pressure where the metastable density value obtained from the extremum condition for the grand potential ceases to be a minimum. To find the limits of stability also for $T < T_{tr}$, we must study the stability of the mean field solution for the liquid phase not only with respect to the gas phase [i.e., along the $n_A = n_B$ line as calculated from Eq. (12)], but also with respect to states with n_A different from n_B.[28] The limit of stability of the liquid is obtained by calculating the determinant of the Hessian for the grand potential and locating the pressures and temperatures where it approaches zero from above,

$$\frac{\partial^2\Omega}{\partial n_A^2}\frac{\partial^2\Omega}{\partial n_B^2}-\left(\frac{\partial^2\Omega}{\partial n_A \partial n_B}\right)^2=0. \tag{14}$$

For the liquid phase (with $n_A = n_B$), the two solutions of (14) for the densities at the spinodal are

$$n_{\pm}=\frac{1}{2}\left[1+\left(1-\frac{2k_BT}{z(J_2\pm J_1)}\right)^{1/2}\right]. \tag{15}$$

The solution n_+ corresponds to the limit of stability with respect to the gas phase [and coincides with the solution calculated directly from Eq. (12) for temperatures other than T_c], while the solution n_- corresponds to the limit of stability with respect to the solid phase. Using these solutions in the expression for the equilibrium pressure (11), we obtain the corresponding expressions for the spinodal values of pressure. We see from Eqs. (11) and (15) that the liquid–gas spinodal pressure would be nonmonotonic, since $2k_BT/(J_1 + J_2)$ is nonmonotonic. As discussed in Sec. IV, the nonmonotonicity in $2k_BT/(J_1 + J_2)$ also leads directly to the existence of the density maximum. Thus, in the present model, the presence of density maxima and the reentrance of the spinodal are intimately related.

Figure 4(b) shows these two spinodals in the P–T plane. Note that they meet tangentially at T_{tr}. We find that the liquid–gas spinodal is the limit of stability above T_{tr}, while the liquid–solid spinodal is the limit of stability below T_{tr}.[29] We see that the liquid–gas spinodal is reentrant and varies nonmonotonically with temperature, exhibiting an extreme value at a finite temperature.

Next, we study the locus of points where the density is maximum. Figure 5 shows the line of density maxima, together with the spinodal lines and the coexistence lines. We see that the end points of the line of density maxima meet the liquid–solid spinodal at the upper end, and the liquid–gas spinodal at the reentrance point. This is consistent with the predictions of Speedy and Debenedetti,[4,5] based on thermodynamic consistency. At the lower end, the slope of the liquid–gas spinodal is changed when the line of density maxima meets the spinodal. At the upper

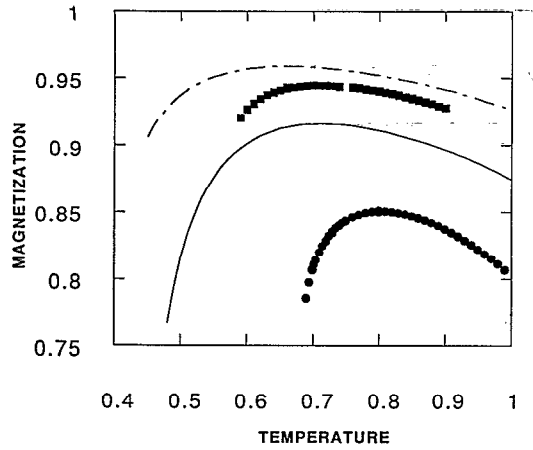

FIG. 6. Magnetization at two constant magnetic field values, $h=0$ (solid curve and filled circles) and $h=0.2$ (dashed curve and filled squares). The continuous lines in the figure are mean field results and the data points are from Monte Carlo simulation. Note that the qualitative behavior of the Monte Carlo simulation is the same as that of the mean field calculation.

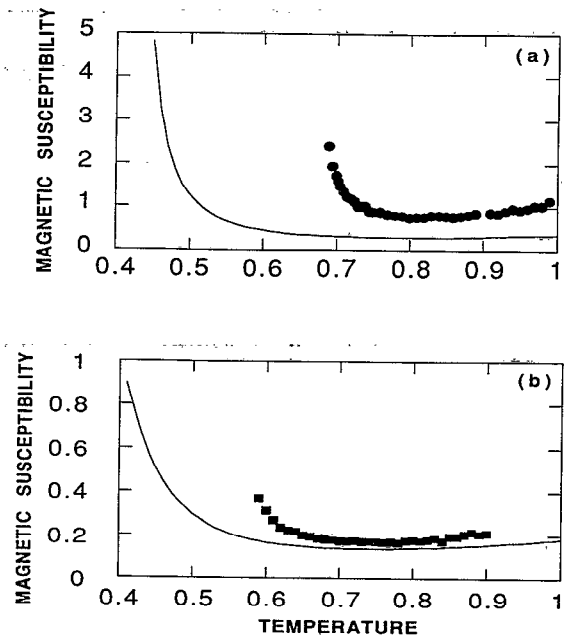

FIG. 7. Magnetic susceptibility from the mean field calculation (continuous lines) and Monte Carlo simulations (data points) for (a) magnetic field $h = 0$ and (b) magnetic field $h = 0.2$. As in Fig. 8, we see qualitative agreement between mean field and Monte Carlo results. Note that the magnitude of the susceptibility is lower for the higher magnetic field value.

end, the liquid–solid spinodal and line of density maxima meet at $T=0$. The high pressure termination of the density maximum line is again consistent with the prediction of Speedy and Debenedetti.

VI. NUMERICAL SIMULATIONS

We have studied the model in the mean field approximation in order to obtain the most detailed information about the system in the metastable region. We have done so, however, on the basis of prior research on the behavior of the system in various limits which shows that the mean field approximation can be relied upon to exhibit the correct qualitative behavior. To obtain an indication of the quantitative accuracy of the mean field approximation, we performed Monte Carlo simulations of the Ising model (which corresponds to the present lattice-gas model) in three dimensions.[30]

In Fig. 6 we show the variation of magnetization with temperature obtained from mean field calculations and Monte Carlo simulations of the three-dimensional model for two different constant field values. Figure 7 shows the magnetic susceptibility at constant field for the same values of the field. Note that in their qualitative trends the simulation results are similar to the corresponding mean field results. The simulations also reproduce the phase diagram calculated obtained from the mean field approximation. As expected, however, the critical point for the ferromagnetic transition is overestimated by the mean field approximation.

To confirm the reentrance behavior and the continuity of the limits of stability of the liquid phase, we performed simulations in the metastable regime for the corresponding Ising model. We determined the limits of stability by defining an arbitrary criterion for the lifetime of the metastable phase (50 Monte Carlo steps). The locus of the limits of stability (or, more accurately, the locus of homogeneous nucleation points) thus obtained is shown in Fig. 8, along with the corresponding mean field solution. It is evident that the limit of stability curve is reentrant, and forms a continuous boundary. We can further distinguish the nature of the limit of stability points by studying the phase to which the system decays when these limits are reached. The simulations confirm the statement above that below

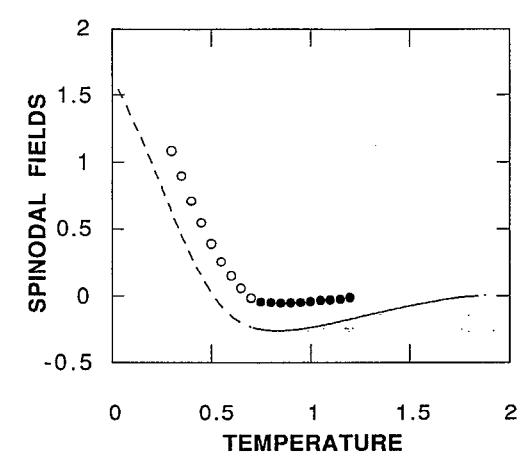

FIG. 8. Spinodal lines from the mean field calculation (continuous lines) and homogeneous nucleation points from Monte Carlo simulations (data points). Note that the nucleation points from the simulations track the mean field spinodal. Also, at temperatures for which the liquid–solid spinodal is the limit of stability, the system nucleates to the solid phase, while at higher temperatures the spinodal and the nucleation are to the gas phase. The open circles indicate nucleation events to the solid phase and filled circles to the gas phase.

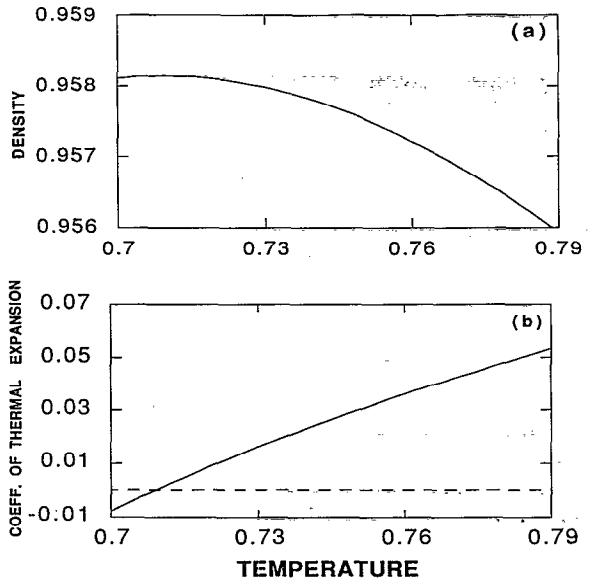

FIG. 9. (a) Density change at constant pressure. (b) Corresponding behavior of the coefficient of thermal expansion, which changes sign at the temperature of maximum density.

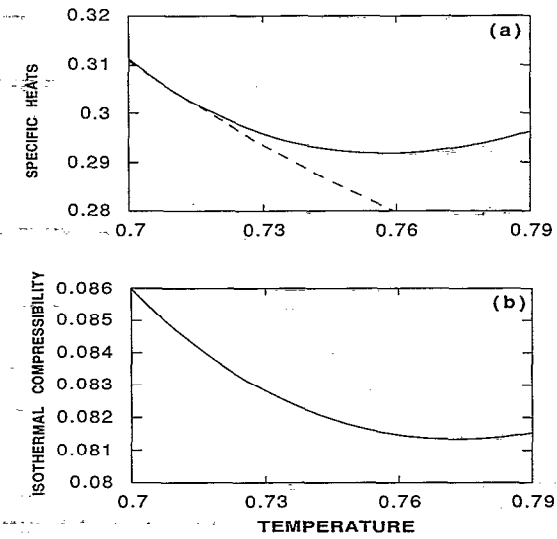

FIG. 10. (a) Specific heats at constant pressure (solid curve) and constant volume (dashed curve) along a constant pressure trajectory. Note that the specific heats increase upon lowering temperature and coincide at the temperature of maximum density from Fig. 9. (b) Isothermal compressibility along a constant pressure trajectory, which increases upon cooling—displaying anomalous behavior.

T_{tr} the limit of stability is the liquid–solid spinodal, while above T_{tr} the limit of stability is the liquid–gas spinodal.

VII. RESPONSE FUNCTIONS

The anomalies of water are described in terms of well known "anomaly indicators." Apart from the density, these indicators are the various response functions one can study and measure. We now present mean field results for specific heats at constant volume and pressure, the isothermal compressibility and the coefficient of thermal expansion. Figure 9(a) shows the density change for a constant pressure trajectory, while Fig. 9(b) shows the corresponding coefficient of thermal expansion. We observe that the model displays a density maximum or, equivalently, a region with negative coefficient of thermal expansion. Figure 10(a) shows the behavior of the specific heats and Fig. 10(b) the isothermal compressibility. The compressibility is nonmonotonic, increases on cooling, and decreases on compression. Although the *qualitative* behavior of these response functions is correct, they do not agree *quantitatively* with experimental values. The density of the liquid phase compared to the density of the open ordered structure is very different from the experimental ratio.

These quantitative discrepancies are common for lattice models and other simplified models.[31] However, the main feature of our model is that it exhibits the correct *anomalous* behavior for water. Further, where comparisons can be made, simulations confirm our mean field results.

The "critical" properties at the supercooling or liquid–solid limit of stability found in the present model are different from the properties near the superheating or liquid–gas limit of stability. In particular, there are no divergences in the isothermal compressibility near the liquid–solid spinodal. When the liquid becomes unstable with respect to the gas phase, there are divergences. This can be understood in terms of the nature of the instabilities at the two spinodals:

(i) At the *liquid–gas spinodal*, the liquid state becomes unstable with respect to the gas along a direction of changing density. The derivative of the pressure with respect to density approaches zero at the liquid–gas spinodal, resulting in divergent compressibility.

(ii) At the *liquid–solid spinodal*, the liquid becomes unstable with respect to "crystal ordering," along a direction orthogonal to density. The derivative of the pressure becomes zero along this orthogonal direction and hence the vanishing of the density derivative does not define the liquid–solid spinodal. Thus, the compressibility does not diverge.

In the temperature range between the lower liquid–gas critical point and T_{tr}, the system becomes unstable with respect to the solid phase. Nevertheless, by extrapolating data to where response functions diverge, the liquid–gas spinodal "hidden behind it" can be deduced as the source of anomalies.

VIII. CONCLUSIONS

We have proposed a lattice model with behavior qualitatively similar to that of water. We focused on the behavior of the spinodal limits to the liquid state, and the relation of these limits to the line of density maxima—topics that have not been addressed sufficiently in previous lattice model studies. We showed that the liquid–gas spinodal is reentrant, and the line of density maxima meets the spinodal at the point of reentrance (as required by thermodynamic consistency). We found that the metastable liquid

state is bounded by a spinodal at positive pressures as well as negative pressures. However, in the present model, the positive pressure spinodal is the limit of stability with respect to the solid state. The two spinodals form a continuous locus, but the "critical" properties of these two spinodals are quite different. While the response functions (specific heat, compressibility) diverge at liquid–gas spinodal, at the liquid–solid spinodal they do not, even though they tend to higher values in the same fashion as occurs near a liquid–gas spinodal.

To our knowledge, the present model exhibits the first example of a liquid–gas spinodal that extends to positive pressures. We emphasize, however, that the physically relevant instability of the liquid upon supercooling is the liquid–solid spinodal. Thus, the supercooling instability in the present model, while consistent with known experimental results, is qualitatively different from those instabilities for which divergences in response functions are predicted.[4]

The present model explicitly demonstrates an intimate relation between the reentrant spinodal and density maximum behavior. Both originate from the contribution of orientational degrees of freedom to the thermodynamics of the system. The present model also takes into account many essential microscopic features of water. By systematic improvement, it should be possible to achieve better accuracy of description. We have studied this model as a first step toward understanding the interrelation between the microscopic mechanisms leading to anomalous behavior and the associated thermodynamic anomalies.

In particular, the transition at high pressures to high density forms of ice should be reproducible within the framework introduced here. It is conceivable that such transitions would be present as ordering transitions of the orientational degrees of freedom in a modified model with interactions between orientational variables. Such a transition has been observed in a previous model, but the transition was found to be of second order.[8] In future studies, we intend to address this and related questions pertaining to quantitative comparisons with water.

In order to further test the utility of the present approach, we will perform simulations of the full Hamiltonian, including orientational degrees of freedom, to study the dynamics of the system. The properties that can be investigated with such simulations are (i) the lifetimes of hydrogen bonds and the restructuring of the hydrogen bond network,[32] (ii) the diffusional behavior, both translational and rotational (these can be studied through the calculation of time correlations of appropriate quantities),[33] and (iii) the fluctuations in energy.[12,34]

An important connection that can be made through a further study of this model is with the percolation picture of anomalous behavior.[15,35] The liquid–solid limit of stability occurs with respect to crystalline ordering. This corresponds to an increase in clusters of four-coordinated sites[15] as the spinodal is approached, suggesting that there would indeed be a percolation transition at the liquid–solid spinodal. The clarifications made earlier regarding the divergent behavior of response functions at the liquid–solid spinodal would then apply to a percolation picture of anomalies as well, independently of the particular model presented here.

ACKNOWLEDGMENTS

We thank A. Angell, S. S. Borick, P. G. Debenedetti, U. Essmann, M. F. Gyure, S. Havlin, H. Larralde, V. Martorana, P. H. Poole, R. J. Speedy, S. Schwarzer, and B. Stošić for helpful discussions and comments on the manuscript. S.S. thanks Robert Putnam of Thinking Machines Corp. for help in computations done on the CM-2, and the Center for Computational Physics at Boston University for computational facilities. F.S. acknowledges the support of Regione Autonoma Sardegna. This work has been supported by British Petroleum and the National Science Foundation. This work is based on the Ph.D. thesis of Srikanth Sastry.

[1] C. A. Angell, in *Water: A Comprehensive Treatise*, edited by F. Franks (Plenum, New York, 1981), Vol. 7, Chap. 1; Ann. Rev. Phys. Chem. **34**, 593 (1983).
[2] J. L. Green, D. J. Durben, G. H. Wolf, and C. A. Angell, Science **249**, 649 (1990).
[3] R. J. Speedy and C. A. Angell, J. Chem. Phys. **65**, 851 (1976).
[4] R. J. Speedy, J. Phys. Chem. **86**, 982 (1982); **86**, 3002 (1982); **91**, 3354 (1987).
[5] P. G. Debenedetti and M. C. D'Antonio, J. Chem. Phys. **84**, 3339 (1986); **85**, 4005 (1986); M. C. D'Antonio and P. G. Debenedetti, *ibid.* **86**, 2229 (1987); P. G. Debenedetti and M. C. D'Antonio, AIChE. J. **34**, 447 (1988).
[6] P. H. Poole, F. Sciortino, U. Essmann, and H. E. Stanley, Nature **360**, 324 (1992).
[7] P. D. Fleming III and J. H. Gibbs, J. Stat. Phys. **10**, 157 (1974); **10**, 351 (1974). A model based on ideas of correlated-site percolation is C.-K. Hu, J. Phys. A **16**, L321 (1983).
[8] G. M. Bell and D. A. Lavis, J. Phys. A **3**, 427 (1970); G. M. Bell, J. Phys. C **5**, 889 (1972); G. M. Bell and D. W. Salt, Trans. Faraday Soc. II **72**, 76 (1976); P. H. E. Meijer, R. Kikuchi, and P. Papon, Physica A **109**, 365 (1981); P. H. E. Meijer, R. Kikuchi, and Eddy Van Royen, Physica A **115**, 124 (1982).
[9] For exceptions, see P. G. Debenedetti, V. S. Raghavan, and S. S. Borick, J. Phys. Chem. **95**, 4540 (1991); M. Sasai, J. Chem. Phys. **93**, 7329 (1990). Debenedetti *et al.* study the limits of stability for a lattice model for a core softened fluid with density anomalies. Sasai studies a lattice model for water.
[10] E. Grünwald, J. Am. Chem. Soc. **108**, 5719 (1986); A. H. Narten and H. A. Levy, Science **165**, 447 (1969); L. Bosio, S. H. Chen, and J. Teixeira, Phys. Rev. A **27**, 1468 (1983); S. Krishnamurthy, R. Bansil, and J. Wiafe-Akenten, J. Chem. Phys. **79**, 5863 (1983); P. A. Giguère, *ibid.* **87**, 4835 (1987); G. E. Walrafen, M. S. Hokmabadi, W.-H. Yang, Y. C. Chu, and B. Monosmith, J. Phys. Chem. **93**, 2909 (1989).
[11] A. Geiger, P. Mausbach, and J. Schnitker, in *Water and Aqueous Solutions*, edited by G. W. Neilson and J. E. Enderby (Adam Hilger, Bristol, 1986); A. Geiger, A. Rahman, and F. H. Stillinger, J. Chem. Phys. **70**, 273 (1979); A. Geiger and P. Mausbach, in *Hydrogen Bonded Liquids*, edited by J. Dore and J. Teixeira (Kluwer Academic, Dordrecht, 1990).
[12] H. Tanaka and I. Ohmine, J. Chem. Phys. **87**, 6128 (1987); I. Ohmine, H. Tanaka, and P. G. Wolynes, *ibid.* **89**, 5852 (1988); H. Tanaka and I. Ohmine, *ibid.* **91**, 6318 (1989).
[13] F. H. Stillinger and A. Rahman, J. Chem. Phys. **60**, 1545 (1974); M. Mezei and D. L. Beveridge, *ibid.* **74**, 622 (1981); R. J. Speedy, J. D. Madura, and W. L. Jorgensen, J. Phys. Chem. **91**, 909 (1987); D. A. Zichi and P. J. Rossky, J. Chem. Phys. **84**, 2814 (1986).
[14] F. Sciortino, A. Geiger, and H. E. Stanley, Phys. Rev. Lett. **65**, 3452 (1990); Nature **354**, 218 (1991); J. Chem. Phys. **96**, 3857 (1992); F. Sciortino, in *Correlations and Connectivity*, edited by H. E. Stanley and N. Ostrowsky (Kluwer Academic, Dordrecht, 1990).
[15] H. E. Stanley and J. Teixeira, J. Chem. Phys. **73**, 3404 (1980); H. E.

Stanley, J. Teixeira, A. Geiger, and R. L. Blumberg, Physica A **106**, 260 (1981).

[16] F. H. Stillinger, Science **209**, 451 (1980).

[17] R. J. Speedy, J. Phys. Chem. **88**, 3364 (1984); **89**, 171 (1985).

[18] Each site has $2z$ neighbors, z of which are on the same sublattice and z on the other sublattice. For both the square lattice and the bcc lattice which we describe later, $z=4$.

[19] The second term in the Hamiltonian defines an interaction energy between occupied and unoccupied sites. This is demanded by the fact that the interaction energy for a hydrogen bond cannot be defined solely in terms of occupancies of bonding sites, since the presence of molecules in the immediate neighborhood affects hydrogen bonding. With only two body interaction terms, part of the hydrogen bond energy has to be defined indirectly. However, the second term of the Hamiltonian in (1) can be rewritten to have finite energies for occupied pairs only, instead of pairs of occupied and empty sites. This would correspond, in the resulting partition function, to a shift in the chemical potential.

[20] The physical features listed at the beginning of this section can be expressed via Hamiltonians that are different from (2). However, such other Hamiltonians should result in qualitatively similar behavior. Our choice has been motivated by the clarity with which the influence of various features in the Hamiltonian can be studied. Also, the essential contribution of orientational entropy to phase behavior is to make higher local density contributions favorable at high temperatures; the Hamiltonian (2) achieves this.

[21] Here, k_B is the Boltzmann constant. Where numerical values are assigned to temperature, k_BT is expressed in units of J.

[22] In all cases, there is an increase in configurational entropy since these excitations can occur on any of the available sites. This increase is the same for all three cases.

[23] This approximation corresponds to truncating the cluster or graph expansion for the partition function. Considering AB interactions only, we expand the Boltzmann factor in the partition function sum as a series. Truncating this series and summing over the Potts variables, we then compared it with the corresponding series expansion for an effective lattice-gas interaction. From this comparison, we obtain the the expression for the AB interaction strength shown in Eq. (4). For details on the validity of such approximations, see Ref. 24.

[24] R. E. Goldstein and J. S. Walker, J. Chem. Phys. **78**, 1492 (1983). A detailed study of lattice-gas theories for systems with lower critical points has been made by these authors and C. A. Vause with models similar to the one presented in this paper, see J. S. Walker and C. A. Vause, Phys. Lett. A **79**, 421 (1980); C. A. Vause and J. S. Walker, *ibid.* **90**, 419 (1982); J. S. Walker and C. A. Vause, J. Chem. Phys. **79**, 2660 (1983); R. E. Goldstein, *ibid.* **79**, 4439 (1983).

[25] J. M. Kincaid and E. G. D. Cohen, Phys. Rep. **22**, 57 (1975); I. D. Lawrie and S. Sarbach, in *Phase Transitions and Critical Phenomena*, edited by C. Domb and J. L. Lebowitz (Academic, New York, 1984), Vol. 9.

[26] For finite values of the magnetic field (which is related to the chemical potential by the mapping of these two models), the boundary between this AF and the paramagnetic phase can be of first order or second order. The transition is of second order above the "tricritical point" and first order below it. In our system, at all temperatures below T_{tr}, the transition to antiferromagnetic ordering is first order and hence we do not discuss tricritical behavior any further.

[27] Experimentally, one observes the relapse to the normal positive slope of the solid–liquid equilibrium line at high pressures. In our model this is not seen. But this is in accordance with the fact that our model does not exhibit the higher density ice forms which coexist with the liquid phase along the solid–liquid line at high pressures. We address this question further in the last section.

[28] Since the grand potential is defined as a surface, the liquid state can become unstable not only with respect to density (i.e., along $n_A = n_B$), but also with respect to sublattice ordering.

[29] In the range of temperatures between T_{tr} and the lower liquid–gas critical point, the liquid–gas solution for the spinodal [shown in Fig. 4(b)] is below the physical limit of stability. However, states defined only along $n_A = n_B$ would be stable till the liquid–gas spinodal solution is reached, with the compressibility diverging along that line. We shall come back to this point when we discuss response functions in Sec. VII.

[30] The Ising model is obtained by defining "spin" variables $S_i \equiv 2n_i - 1$, and expressing the grand canonical partition function (6) in terms of the spin variables. This partition function thus expressed defines a canonical partition function for an Ising system in a magnetic field, with the Hamiltonian,

$$\mathcal{H}_{\text{Ising}} = -(J_1/2)\sum_{\langle ij\rangle}^{AB} S_iS_j - (J_2/2)\sum_{\langle ik\rangle}^{AA} S_iS_k - h\sum_i S_i,$$

with the magnetic field h given in terms of the chemical potential. We treat the field as an independent variable.

[31] L. W. Dahl and H. C. Andersen, J. Chem. Phys. **78**, 1980 (1983).

[32] F. Sciortino and S. L. Fornili, J. Chem. Phys. **90**, 2786 (1989); F. Sciortino, P. H. Poole, H. E. Stanley, and S. Havlin, Phys. Rev. Lett. **64**, 1686 (1990).

[33] D. Bertolini, M. Cassettari, and G. Salvetti, J. Chem. Phys. **76**, 3285 (1982); E. Lang and H. D. Lüdemann, Angew. Chem. I. Ed. **21**, 315 (1982).

[34] I. Ohmine and H. Tanaka, J. Chem. Phys. **93**, 8138 (1990); M. Sasai and I. Ohmine and R. Ramaswamy, *ibid.* **96**, 3045 (1992).

[35] Hu (Ref. 7) has developed an explicit interaction Hamiltonian for hydrogen bonding in water molecules, and expressed this as a generating function of a bond-correlated percolation model.